

A Study on Airfoil Design for Future Mars Airplane

Akira Oyama* and Kozo Fujii†
JAXA/ISAS, Sagami-hara, Kanagawa, 229-8510, Japan

An optimum airfoil design for future Mars airplane for Mars exploration is obtained by evolutionary computation coupled with a two-dimensional Reynolds-averaged Navier-Stokes solver. The optimized airfoil design is also compared with other airfoil designs optimized at different Reynolds number or at different Mach number to discuss Reynolds number and Mach number effects on airfoil design. These results indicate same important design policies in airfoil design optimization in regard to Reynolds number and Mach number effects.

Nomenclature

C_d	=	total drag coefficient
$C_{d\text{ pressure}}$	=	pressure drag coefficient
$C_{d\text{ viscous}}$	=	viscous drag coefficient
C_l	=	lift coefficient
C_p	=	surface pressure coefficient
c	=	chord length
D	=	drag
L	=	lift
M	=	Mach number
Re	=	Reynolds number
x	=	chordwise coordinate
y	=	coordinate normal to the chord

I. Introduction

JAPAN Aerospace Exploration Agency (JAXA) has been actively exploring the solar system by its unique approach. Currently, HAYABUSA is approaching to an asteroid to bring back samples of an asteroid's surface to earth. Also, the Venus Climate Orbiter project (PLANET-C), the third Japanese solar physics satellite project (SOLAR-B), the Japanese lunar satellite (SELENE) and penetrator (LUNAR-A) projects, and the joint Mercury exploration project between Japan and Europe (BepiColombo) are ongoing. As in JAXA long-term visions¹ announced in April 2005, JAXA is aiming at further exploration of the solar system in the next 20 years. Mars exploration by an aircraft is an idea presented in the long-term visions of JAXA and has been discussed in Institute of Space and Astronautical Science (ISAS) for almost two years.

Current and previous missions to Mars base on ground-based rovers and orbiters. Rovers provide detailed data on the surface but their reach is limited to a very small area. On the other hand, orbiting sensors provide large spatial coverage but resolution of the measured data is very low. Therefore, aircraft mission on Mars is expected to provide very interesting information as an aircraft can get high-resolution data of atmosphere and surface of Mars over a very large region.

Among many options for Mars exploration by an aircraft such as balloon, helicopter, and flapping wing, airplane with fixed wing has some advantages over other options such as larger spatial coverage, controllability, reliability, and cost. In fact, aircraft missions to Mars discussed in U.S.²⁻⁴ base on airplane with fixed wing.

The optimal airplane design for Mars exploration, however, may be very different from the conventional airplanes on Earth. First, Reynolds number of Mars airplane becomes smaller ($Re=10^5$) than flow condition of typical airplanes on Earth ($Re=10^7$) because the air on Mars is very thin compared with the air on Earth and the airplane size is constrained to be small due to its launcher capability. Second, its cruising Mach number becomes high because speed of sound on Mars is smaller than that on Earth (roughly 2/3) and the aircraft needs a certain

* Research Associate, Department of Space Transportation Engineering, 3-1-1 Yoshinodai, Member AIAA.

† Professor, Department of Space Transportation Engineering, 3-1-1 Yoshinodai, Fellow AIAA.

cruising speed to gain sufficient dynamic pressure in the thin atmosphere. Because aircrafts flying in such flow condition on Earth is limited to high-altitude airplanes, optimum design of Mars airplane is not well known.

Therefore, objectives of the present study are to obtain an optimum airfoil shape for Mars airplane and to discuss Reynolds number and Mach number effects on the optimum airfoil design by comparing the airfoil designs optimized at different Reynolds number and Mach numbers.

II. Formulation of the Design Problem

The airplane designed for future geographical exploration on Mars in Japan⁵ (Fig. 1) is considered in this study. Mach number and Reynolds number of the airplane at the cruising condition are roughly 0.48 and 10^5 , respectively. The objective of the present airfoil design problem is maximization of the lift-to-drag ratio at its cruising condition. In the present study, the cruising Mach number and angle of attack are assumed to be 0.4735 and two degrees, respectively. Reynolds number is set to 10^5 based on the Mars air properties and reference length of the root chord. Turbulent flow is assumed. No thickness constraint is posed to see pure aerodynamic characteristics of the airfoil shape.

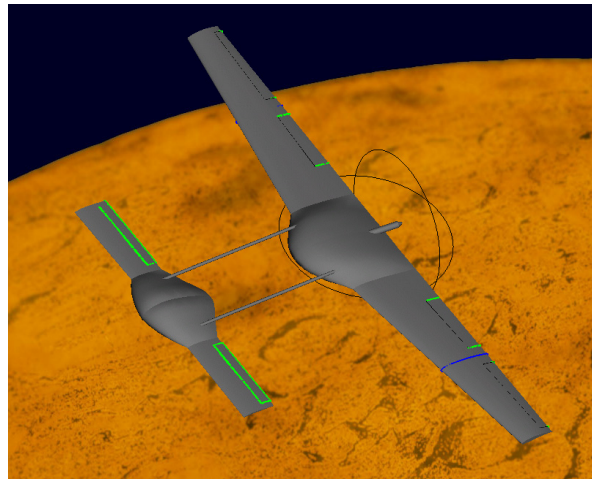


Figure 1. A design of airplane for Mars exploration.

III. Approach

A. Airfoil Shape Parameterization

Selection of a parameterization technique is an important step for airfoil shape design optimization⁶. Here, the B-Spline curves are used for the airfoil shape parameterization. The parameterization based on the B-Spline has advantages such as 1) second-order derivative is continuous, 2) various airfoil shapes can be expressed with small number of design parameters, and 3) definition of initial design space is intuitive. In this study, nine control points are used to control the B-Spline curves (Fig.2) where number of the control points is determined according to the authors' experience in high-Reynolds number airfoil design optimization. Because the control points at the leading and trailing edges are fixed, number of the control points to be optimized is six. The design parameters are the x and y coordinates of the six control points. Total number of design parameters is twelve. The airfoil shape represented by the B-Spline curves are modified so that the airfoil shape passes $(0,0)$ and $(1,0)$.

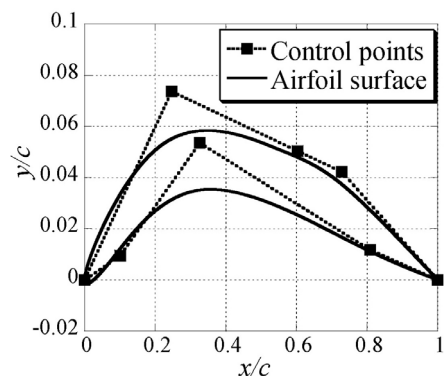


Figure 2. Airfoil shape parameterization based on the B-Spline curves.

B. Evolutionary Algorithm

Evolutionary algorithms (EAs, for example, see reference⁷) are emergent optimization algorithms mimicking mechanism of the natural evolution, where a biological population evolves over generations to adapt to an environment by selection, recombination and mutation. When EAs are applied to optimization problems, fitness, individual and genes usually correspond to an objective function value, a design candidate, and design variables, respectively. One of the key features of EAs is that they search from multiple points in the design space, instead of moving from a single point like gradient-based methods do. Furthermore, these methods work on function evaluations alone and do not require derivatives or gradients of the objective function. These features lead to the following advantages:

- 1) Robustness: EAs have capability of finding a global optimum, because they don't use function gradients that direct the search toward an exact local optimum. In addition, EAs have capability to handle any design problems that may involve non-differentiable objective function and/or a mix of continuous, discrete, and integer design parameters.
- 2) Suitability to parallel computing: Since EAs are population-based search algorithms, all design candidates in each generation can be evaluated in parallel by using the simple master-slave concept. Parallel efficiency is also very high, if objective function evaluations consume most of CPU time. Aerodynamic optimization using Computational Fluid Dynamics (CFD) is a typical case.
- 3) Simplicity in coupling CFD codes: As these methods use only objective function values of design candidates, EAs do not need substantial modification or sophisticated interface to the CFD code. If an all-out re-coding were required to every optimization problem, like the adjoint methods, extensive validation of the new code would be necessary every time. EAs can save such troubles.

Owing to the above advantages over the analytical methods, EAs have become increasingly popular in a broad class of design problems⁸.

In this paper, real-coded adaptive range genetic algorithm⁹ (ARGA) was used. The real-coded ARGA is a robust and efficient EA that is developed by incorporating the idea of the dynamic coding and floating-point representation. The read-coded ARGA solves large-scale design optimization problems very efficiently by promoting the population toward promising design regions during the optimization process (Fig. 3). For detail, see the reference⁹.

The present ARGA adopts the elitist strategy¹⁰ where the best and the second best individuals in each generation are transferred into the next generation without any recombination or mutation. The parental selection consists of the stochastic universal sampling¹¹ and the ranking method using Michalewicz's nonlinear function¹². Blended crossover¹³ (BLX-0.5) is used for recombination. Mutation takes place at a probability of 10% and then adds a random disturbance to the corresponding gene up to 10% of the given range of each design parameter. The population size is kept at 64 and the maximum number of generations is set to 100. The initial population is generated randomly over the entire design space. Evaluation process at each generation was parallelized using the master-slave concept; the grid generations and the flow calculations associated to the individuals of a generation were distributed into 32 processing elements of the JAXA/ISAS NEC SX-6 computing system. This made the corresponding turnaround time almost 1/32 because the CPU time used for EA operators are negligible. Turn around time of each optimization was roughly two hours.

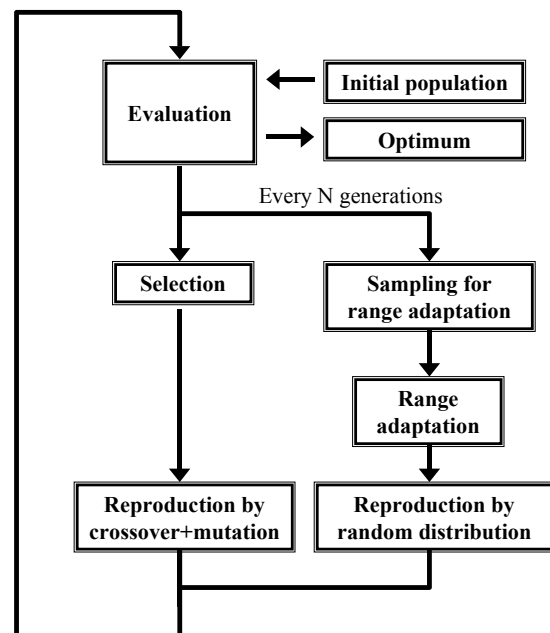


Figure 3. Flow chart of the real-coded ARGA.

C. Aerodynamic Evaluation

The flow physics can be represented by a wide range of approximations. Although a Reynolds-averaged Navier-Stokes calculation is computationally expensive, the two-dimensional Navier-Stokes equations must be solved for the present aerodynamic airfoil shape design optimization because flows around an airfoil at the present flow condition involve significant viscous effects such as potential boundary-layer separations. In this paper, a two-dimensional thin-layer Reynolds-averaged Navier-Stokes solver is used to guarantee an accurate model of the flow field.

The present grid generator algebraically creates a C-type grid (201 grid points in chordwise direction, 49 grid points in normal direction) for each design candidate. The present Navier-Stokes code employs total variation diminishing type upwind differencing¹⁴, the lower-upper symmetric Gauss-Seidel scheme¹⁵ and Baldwin-Lomax turbulent model. The multigrid method¹⁶ and space variable time step is employed for convergence acceleration.

IV. Results

A. Airfoil Design Optimization at the Cruising Condition of the Mars Airplane

To get an idea what is an optimum airfoil shape at low Reynolds number and high Mach number flow condition, an optimum airfoil shape is obtained by the evolutionary computation coupled with the Navier-Stokes solver for the Mars Airplane at its cruising condition (Mach number of 0.4735 and Reynolds number of 10^5). Objective of the optimization problem is lift-to-drag ratio at angle of attack of 2 degrees. Figure 4 shows the optimized airfoil and Mach number and pressure contours of the flow. The optimized airfoil shape has very thin airfoil thickness and strong camber to enhance expansion under the airfoil and compression above the airfoil. As a result, the optimized airfoil has large lift. Increase in camber is limited by increase in drag due to large flow separation or generation of shock wave.

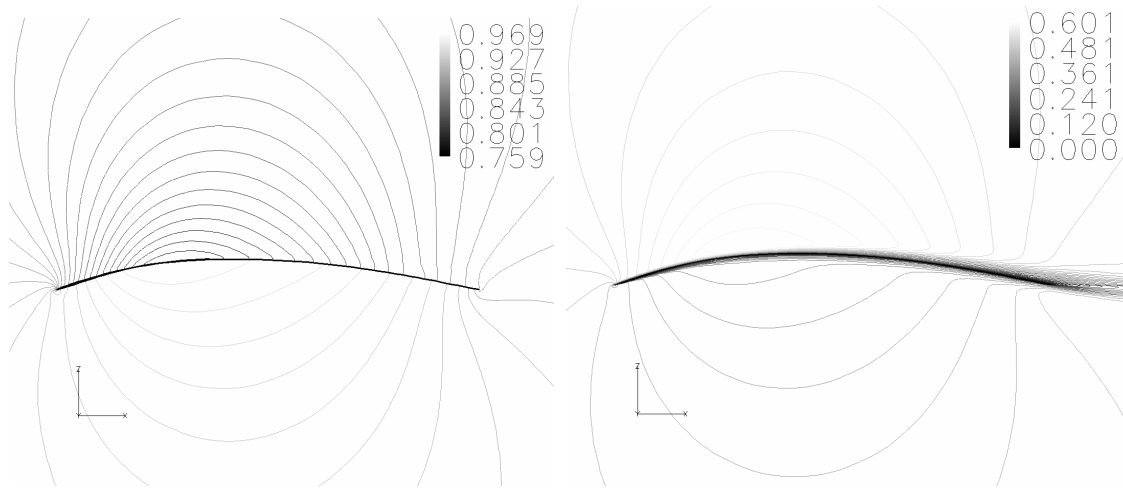


Figure. 4 Pressure (left) and Mach number (right) contours of the optimized airfoil shape.

B. Discussion on Reynolds Number Effect

The optimized airfoil at Reynolds number of 10^5 (Mars airplane flight condition) and the optimized airfoil at Reynolds number of 10^7 (flight condition of typical airplanes on Earth) are compared to discuss Reynolds number effect on aerodynamic airfoil shape design. Figure 5 compares these two airfoils. While the optimized airfoil at Reynolds number of 10^5 has extremely thin airfoil thickness, the optimized airfoil at Reynolds number of 10^7 has substantial thickness in the front of the airfoil because a sharp leading edge leads to flow separation near at the leading edge at the high Reynolds number. This figure also indicates that an optimized airfoil design (in the sense of maximization of L/D) at low Reynolds number has large camber to increase lift because of its viscous drag (Fig. 6). Lift-to-drag ratio and lift and drag coefficients of the optimized airfoils are summarized in Table 1.

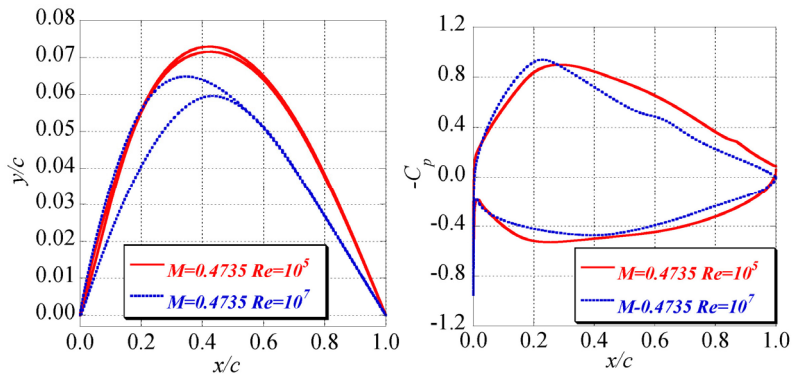


Figure 5. Comparison of the optimum airfoil shapes and corresponding surface pressure distributions.

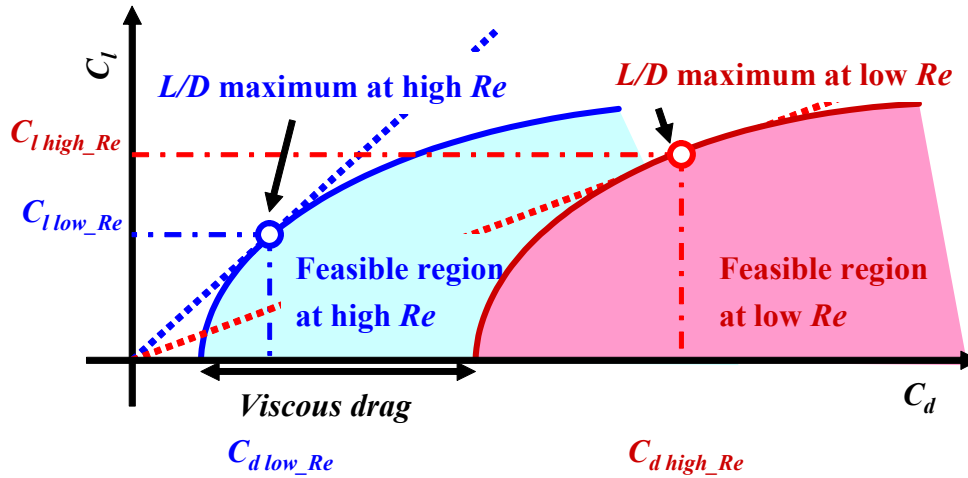


Figure 6. Comparison of L/D maximum designs at different Reynolds number. Feasible region of the optimization problem at lower Reynolds number condition shifts to the right due to the increase in viscous drag. As a result, the L/D maximum design at low Reynolds number has higher lift, higher drag, and smaller L/D than the L/D maximum design at high Reynolds number.

Table 1. Comparison of lift-to-drag ratio and lift and drag coefficients of the optimized airfoils at $M=0.4735$.

	L/D	C_l	C_d	$C_{d\ pressure}$	$C_{d\ viscous}$
Optimized airfoil at $Re=10^5$	40.2	0.977	0.0243	0.0113	0.0130
Optimized airfoil at $Re=10^7$	77.9	0.844	0.0108	0.0061	0.0048

C. Discussion on Mach Number Effect

To discuss Mach number effect on airfoil design optimization, the optimized airfoil for the Mars airplane is compared with the optimized design at the same Reynolds number and higher Mach number of 0.65, which corresponds to the cruising condition of a NASA Mars airplane³. Figure 7 compares these two airfoils. The optimized airfoil at higher Mach number has lower camber to reduce its lift for maximum L/D at high Mach number flow condition (Fig. 8). This airfoil also has round leading edge as the supercritical airfoil.

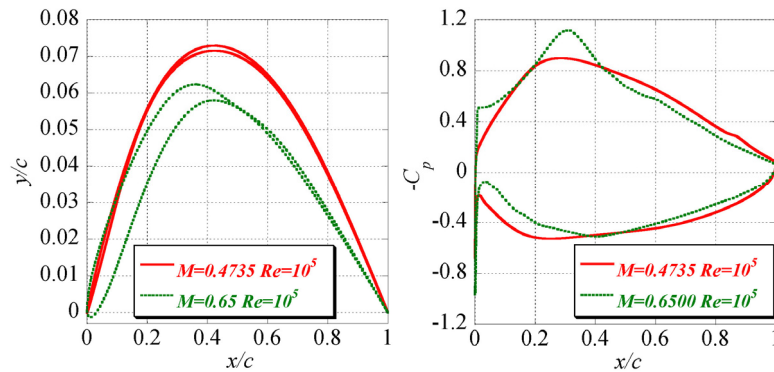


Figure 7. Comparison of the optimum airfoil shapes and corresponding surface pressure distributions.

Lift-to-drag ratio and lift and drag coefficients of the optimized airfoils are summarized in Table 2.

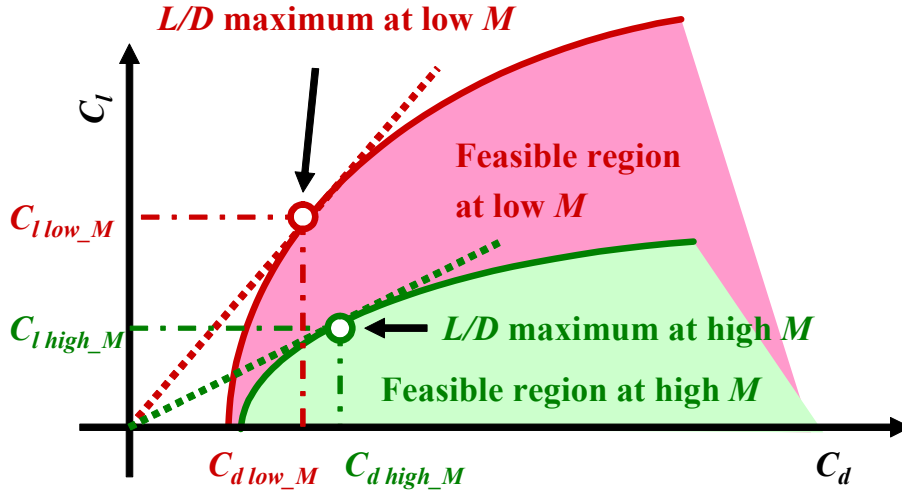


Figure 8. Comparison of L/D maximum designs at different Mach number. Feasible region of the optimization problem at higher Mach number condition is narrower than that of the optimization problem at lower Mach number due to the compressive effect. As a result, the L/D maximum design at high Mach number has lower lift, higher drag, and smaller L/D than the L/D maximum design at lower Mach number.

Table 2. Comparison of lift-to-drag ratio and lift and drag coefficients of the optimized airfoils at $Re=10^5$.

	L/D	C_l	C_d
Optimized airfoil at $M=0.4735$	40.2	0.977	0.0243
Optimized airfoil at $M=0.6500$	36.8	0.925	0.0252

V. Conclusion

An optimum airfoil design for the future Mars airplane for Mars exploration was obtained at low Reynolds number and high Mach number flow condition by evolutionary computation coupled with a two-dimensional Reynolds-averaged Navier-Stokes computation. The optimized airfoil design was also compared with other airfoil designs optimized at different Reynolds number or at different Mach number to discuss the Reynolds number and Mach number effects on airfoil design.

The optimized airfoil in the sense of aerodynamic performance (L/D maximization) at the cruising flow condition has very thin airfoil thickness and strong camber to enhance expansion under the airfoil and compression above the airfoil to get large lift. Increase in camber is limited by increase in drag due to large flow separation or generation of shock wave.

Next, Reynolds number effect on aerodynamic airfoil shape design was discussed by comparing the optimized airfoils at different Reynolds number. While the optimized airfoil at Reynolds number of 10^5 has extremely thin airfoil thickness, the optimized airfoil at Reynolds number of 10^7 has substantial thickness in the front of the airfoil because a sharp leading edge leads to flow separation at the leading edge at high Reynolds number. The comparison also showed that an optimized airfoil design (in the sense of maximization of L/D) at lower Reynolds number has larger camber to increase lift because of its viscous drag.

To discuss Mach number effect on airfoil design optimization, the optimized airfoil for the Mars airplane is compared with the optimized airfoil design at higher Mach number. The optimized airfoil at higher Mach number has lower camber to reduce its lift for maximum L/D . This airfoil also has round leading edge as the supercritical airfoil.

These results indicate some important design policies in airfoil design optimization with regard to Reynolds number and Mach number effects: 1) Optimum airfoil shape in the sense of maximization of L/D at a design point has thin thickness distribution and thus the thickness distribution of an airfoil should be determined according to optimality in other respects such as optimality in structure and control, 2) Optimum leading edge shape depends on

Reynolds number and Mach number of the design condition, 3) Optimum camber distribution also depends on Reynolds number and Mach number of the design condition.

Since the optimum leading edge shape at low Reynolds number is very sharp, optimization with more control points for airfoil shape parameterization may produce a better airfoil design. In the final paper, airfoil shape design optimization with more control points will be demonstrated to get into deeper discussion on Reynolds number and Mach number effects. Also, optimal airfoil shapes for multi-point design will be presented in the final paper.

References

- ¹URL:<http://www.jaxa.jp> [cited 15 May 2005] (currently only in Japanese).
- ²Hall, D. W., Parks, R. W., and Morris, S., "Airplane for Mars Exploration," URL:<http://www.redpeace.org>, [cited 15 May 2005].
- ³Guynn, M. D., Croom, M. A., Smith, S. C., Parks, R. W., and Gelhausen, P. A., "Evolution of a Mars Airplane Concept for the ARES Mars Scout Mission," 2nd AIAA Unmanned Unlimited Systems, Technologies, and Operations, AIAA paper 2003-6578, 2003.
- ⁴Gage, P. J., Allen, G. A. Jr, Park, C, Brown, J. D., Wercinski, P. F., and Tam, T. C., "A Loaf-Shaped Entry Vehicle for a Mars Airplane (The Best Thing Since Sliced Bread?)," 38th Aerospace Sciences Meeting & Exhibit, AIAA Paper 2000-0634, 2000.
- ⁵Tanaka, Y., Okabe, Y., Suzuki, H., Nakamura, K., Kubo, D., Tokuhiko, M., and Rinoie, K., "Conceptual Design of Mars Airplane for Geographical Exploration," Proceedings of the 36th JSASS Annual Meeting, JSASS, Tokyo, 2005, pp. 61-64 (in Japanese).
- ⁶Oyama, A., Obayashi, S., Nakahashi, K., and Hirose, N., "Fractional Factorial Design of Genetic Coding for Aerodynamic Optimization," AIAA Paper 1999-3298, 1999.
- ⁷Deb, K.: *Multi-Objective Optimization using Evolutionary Algorithms*, John Wiley & Sons, New York, 2001.
- ⁸Fonseca, C. M., Fleming, P. J., Zitzler, E., Deb, K., and Thiele, L (Eds.), *Evolutionary Multi-Criterion Optimization*, Springer-Verlag, Berlin, 2003.
- ⁹Oyama, A., Obayashi, S., and Nakamura, T., "Real-Coded Adaptive Range Genetic Algorithm Applied to Transonic Wing Optimization," *Applied Soft Computing*, Vol. 1, No. 3, 2001, pp.179-187.
- ¹⁰De Jong, K. A., "An Analysis of the Behavior of a Class of Genetic Adaptive Systems," Doctoral Dissertation, University of Michigan, Ann Arbor, 1975.
- ¹¹Baker, J. E., "Reducing Bias and Inefficiency in the Selection Algorithm," *Proceedings of the Second International Conference on Genetic Algorithms*, Morgan Kaufmann Publishers, Inc., San Mateo, CA, 1987, pp. 14-21.
- ¹²Michalewicz, Z., *Genetic Algorithms + Data Structures = Evolution Programs*, third revised edition, Springer-Verlag, Berlin 1996.
- ¹³Eshelman, L. J. and Schaffer, J. D., "Real-coded genetic algorithms and interval schemata," *Foundations of Genetic Algorithms.2*, Morgan Kaufmann Publishers, Inc., San Mateo, CA, 1993, pp. 187-202.
- ¹⁴Obayashi, S. and Wada, Y., "Practical Formulation of a Positively Conservative Scheme," *AIAA Journal*, Vol. 32, No. 8, 1994, pp. 1093-1095.
- ¹⁵Yoon, S. and Jameson, A., "Lower-Upper Symmetric-Gauss-Seidel Method for the Euler and Navier-Stokes Equations," *AIAA Journal*, Vol. 26, No. 9, 1988, pp. 1025-1026.
- ¹⁶Jameson, A., "Solution of the Euler Equations for Two-Dimensional Transonic Flow by a Multigrid Method," *Applied Mathematics and Computation*, Vol. 13, 1983, pp. 327-356.